Environment International 185 (2024) 108519

Contents lists available at ScienceDirect

Environment International

journal homepage: www.elsevier.com/locate/envint

Full length article

Variability of ambient air ammonia in urban Europe (Finland, France, Italy, Spain, and the UK)

Xiansheng Liu [a,*], Rosa Lara [a], Marvin Dufresne [b], Lijie Wu [c], Xun Zhang [c,*], Tao Wang [d,*], Marta Monge [a], Cristina Reche [a], Anna Di Leo [e], Guido Lanzani [e], Cristina Colombi [e], Anna Font [b], Annalisa Sheehan [f], David C. Green [f,g], Ulla Makkonen [h], Stéphane Sauvage [b], Thérèse Salameh [b], Jean-Eudes Petit [i], Mélodie Chatain [j], Hugh Coe [k,l], Siqi Hou [m], Roy Harrison [m,n], Philip K. Hopke [o,p], Tuukka Petäjä [q], Andrés Alastuey [a], Xavier Querol [a]

[a] Institute of Environmental Assessment and Water Research (IDAEA-CSIC), Barcelona 08034, Spain
[b] IMT Nord Europe, Institut Mines-Télécom, Univ. Lille, Centre for Energy and Environment, Lille F-59000, France
[c] Beijing Key Laboratory of Big Data Technology for Food Safety, School of Computer Science and Engineering, Beijing Technology and Business University, Beijing 100048, China
[d] Shanghai Key Laboratory of Atmospheric Particle Pollution and Prevention, Department of Environmental Science & Engineering, Fudan University, Shanghai 200433, China
[e] ARPA Lombardia, via Rosellini 17, Milano 20124, Italy
[f] MRC Centre for Environment and Health, Environmental Research Group, Imperial College, London, UK
[g] NIHR HPRU in Environmental Exposures and Health, Imperial College, London W12 0BZ, UK
[h] Finnish Meteorological Institute, Erik Palmenin Aukio 1, Helsinki 00560, Finland
[i] Laboratoire des Sciences du Climat et de l'Environnement, CEA/Orme des Merisiers, Gif-sur-Yvette, France
[j] Atmo Grand Est, 5 Rue de Madrid, Schiltigheim 67300, France
[k] Department of Earth and Environmental Sciences, University of Manchester, Manchester M60 1QD, UK
[l] National Centre for Atmospheric Sciences, University of Manchester, Manchester M60 1QD, UK
[m] School of Geography Earth and Environmental Science, University of Birmingham, Birmingham, UK
[n] Department of Environmental Sciences/Center of Excellence in Environmental Studies, King Abdulaziz University, Jeddah, Saudi Arabia
[o] Department of Public Health Sciences, University of Rochester School of Medicine and Dentistry, Rochester, NY 14642, USA
[p] Institute for a Sustainable Environment, Clarkson University, Potsdam, NY 13699, USA
[q] Institute for Atmospheric and Earth System Research (INAR), Faculty of Science, University of Helsinki, Finland

ARTICLE INFO

Keywords:
Ammonia
Europe
Urban
Temporal variability
Spatial variability

ABSTRACT

This study addressed the scarcity of NH_3 measurements in urban Europe and the diverse monitoring protocols, hindering direct data comparison. Sixty-nine datasets from Finland, France, Italy, Spain, and the UK across various site types, including industrial (IND, 8), traffic (TR, 12), urban (UB, 22), suburban (SUB, 12), and regional background (RB, 15), are analyzed to this study. Among these, 26 sites provided 5, or more, years of data for time series analysis. Despite varied protocols, necessitating future harmonization, the average NH_3 concentration across sites reached 8.0 ± 8.9 μg/m^3. Excluding farming/agricultural hotspots (FAHs), IND and TR sites had the highest concentrations (4.7 ± 3.2 and 4.5 ± 1.0 μg/m^3), followed by UB, SUB, and RB sites (3.3 ± 1.5, 2.7 ± 1.3, and 1.0 ± 0.3 μg/m^3, respectively) indicating that industrial, traffic, and other urban sources were primary contributors to NH_3 outside FAH regions. When referring exclusively to the FAHs, concentrations ranged from 10.0 ± 2.3 to 15.6 ± 17.2 μg/m^3, with the highest concentrations being reached in RB sites close to the farming and agricultural sources, and that, on average for FAHs there is a decreasing NH_3 concentration gradient towards the city. Time trends showed that over half of the sites (18/26) observed statistically significant trends. Approximately 50 % of UB and TR sites showed a decreasing trend, while 30 % an increasing one. Meta-analysis revealed a small insignificant decreasing trend for non-FAH RB sites. In FAHs, there was a significant upward trend at a rate of 3.51[0.45,6.57]%/yr. Seasonal patterns of NH_3 concentrations varied, with urban areas experiencing fluctuations influenced by surrounding emissions, particularly in FAHs. Diel variation showed differing patterns at urban monitoring sites, all with higher daytime concentrations, but with variations in peak

* Corresponding authors.
E-mail addresses: xiansheng.liu@idaea.csic.es (X. Liu), zhangxun@btbu.edu.cn (X. Zhang), wangtao_fd@fudan.edu.cn (T. Wang).

https://doi.org/10.1016/j.envint.2024.108519
Received 27 November 2023; Received in revised form 24 January 2024; Accepted 19 February 2024
Available online 28 February 2024

times depending on major emission sources and meteorological patterns. These results offer valuable insights into the spatio-temporal patterns of gas-phase NH_3 concentrations in urban Europe, contributing to future efforts in benchmarking NH_3 pollution control in urban areas.

1. Introduction

The progressive abatement of primary PM emissions in the last decades, has led to a current urban $PM_{2.5}$ composition dominated by both secondary inorganic and organic aerosols (SIA and SOA) (Amato et al., 2016; Bressi et al., 2021; Chen et al., 2022; In'T Veld et al., 2023a; In'T Veld et al., 2023b). Among the precursors of SIA, ammonia (NH_3), sulfur dioxide (SO_2), and nitrogen oxides (NO_X) are the most relevant. These contribute to formation of PM through gas-to-particle conversion·NH_3 plays an important role in determining the total particle mass and number concentrations, apart from the extent of neutralization of atmospheric PM (Kirkby et al., 2011). These processes lead to the formation of ammonium sulphate and nitrate ($(NH_4)_2SO_4$ and NH_4NO_3), causing increased urban PM exposure and posing a potential threat to human health (Wang et al., 2013; Lelieveld et al., 2015; Van Damme et al., 2018).

In the European Union-27 nations (EU-27) agriculture was the dominant (94 % of the total) contributor in the NH_3 emission inventory in 2020, while industry, road transportation, and solid waste each contributed only 1 % to the overall emissions (EEA, 2022). However, within urban areas of the EU, the contribution of NH_3 derived from traffic sources to atmospheric NH_3 levels may be greater than what is reported in official inventories, due to the widespread implementation of selective catalytic reduction (SCR) NOx-controls in the new diesel vehicles (Hopke and Querol, 2022), which uses urea or NH_3 as catalysts to reduce NO_2 tail-pipe emissions. The fugitive emissions from urban waste management and from sewage systems might also contribute to increase urban NH_3 (Pandolfi et al., 2012; Reche et al., 2012; 2015). Furthermore, despite emissions in $PM_{2.5}$ and PM_{10} concentrations in the EU-27 declined by 30 % and 32 % respectively, from 2005 to 2020 according to inventories, NH_3 emissions underwent a modest reduction, of only 8 % (EEA, 2022). While this reduction meets the Gothenburg Protocol (https://www.unece.org/env/lrtap/multi_h1.htm) target for NH_3 emissions (a 6 % reduction in NH_3 emissions in 2020 compared to 2005), NH_3 remains the pollutant with the smallest percentage reduction, highlighting the urgency of abating its emissions. By using remote sensing data, Van Damme et al. (2021) estimated a roughly 13 % rise in global NH_3 concentrations between 2008 and 2018, of which the growth rate was approximately 6, 3, 2 and 2 % /yr in East Asia, West and Central Africa, North America and Europe, respectively. More recently, Tichý et al. (2023) found that NH_3 emissions peaked in northern Europe due to agricultural application and livestock management and the local maxima were found over western Europe (industrial activity) and over Spain (pig farming). Their calculations show that these emissions decreased by − 26 % from 2013 to 2020 showing that the abatement strategies adopted by the EU have been very efficient.

Unlike $PM_{2.5}$, PM_{10}, SO_2, NO_2, O_3, and CO, NH_3 is currently unregulated by the EU Air Quality Directive without Air Quality Standards. However, a number of Member States set thresholds for the protection of vegetation, or recommended targets are proposed by international bodies (UNECE, 2007; Cape et al., 2009). In many regions of the world, anthropogenic NH_3 emissions are essentially uncontrolled (Shephard et al., 2020). Additionally, measurement of NH_3 concentration is severely limited, with most measurements (offering consistent spatial variations and long-term data) taking place in regional background sites. This reliance on regional background sites can lead to an underestimation of the influence of urban emissions on NH_3 levels in cities, contributing to a deficiency in observational data and substantial uncertainty in our comprehension of urban NH_3 dynamics (Reche et al., 2022). Therefore, it is important to measure urban NH_3 pollution. Monitoring would help gain better understanding of the effects NH_3 have on the formation of PM, but also to provide basic information for mitigation policies (Hopke and Querol, 2022). In order to evaluate the relative roles of different NH_3 sources, there is a need for quantitative mapping of NH_3 concentrations in different environments spanning from urban to rural settings as well as NH_3 hotspots and contrasting background conditions.

In previous studies, most experimental studies and inventories examining NH_3 emissions have focused attention on the agricultural and livestock sources, with extensive results (Sutton et al., 1995; Ni et al., 2000; Sutton et al., 2001; Misselbrook et al., 2004; Hellsten et al., 2008; Gu et al., 2014, Sutton et al., 2022). For instance, in the UK, a large spatial heterogeneity in NH_3 concentrations was observed, with the highest levels in areas with intensive agriculture (up to 22 $\mu g/m^3$). Peak NH_3 concentrations occurred in regions dominated by sheep farming, driven by increased volatilization of NH_3 in warmer summer temperatures (Tang et al., 2018). Sutton et al. (2022) propose a number of key measures to recycle N in agriculture and farming and then to reduce NH_3 emissions. Meanwhile, the estimation of non-agricultural NH_3 sources has become an area of research, especially in urban areas, with management of organic waste, sewage systems, and road traffic emerging as major contributors to NH_3 levels (Pandolfi et al., 2012; Reche et al., 2012; Hopke and Querol, 2022). Using remote sensing, it has been found that NH_3 emissions increased with vehicular miles traveled (VMT) increasing (Frey, 2018). Cold starts had 1.7 times higher than for a fully operational catalyst (Farren et al., 2021). Similarly, SRC systems have been widely implemented in the new diesel vehicles (EURO 6/VI) to meet the stringent emission standards for NO_X by adding-blue that generate NH_3 to reduce NOx ($8NH_3 + 6NO_2 \rightarrow 7\ N2 + 12H_2O$) (Song et al., 2015; Jeon et al., 2016; Hopke and Querol, 2022). In Barcelona, however, Reche et al. (2012) and Pandolfi et al. (2012) found the highest NH_3 concentrations in the old town, with restricted traffic, but a high population density and very narrow streets. They observed exceptionally high concentrations in streets that had a substantial number of organic waste containers in the city. Fagerli et al. (2021) found an increase in ambient NH_3 background concentrations in Europe during the last decade, which was opposite to the slight downward trend of NH_3 emissions, and was attributed to the lower NH_3 consumption to generate $(NH_4)_2SO_4$ and NH_4NO_3 due to the marked decreases in the emissions of SO_2 and NO_x.

RI-URBANS (Research Infrastructures Services Reinforcing Air Quality Monitoring Capacities in European Urban & Industrial Areas, the European Union's Horizon 2020 research and innovation program, 101036245) is a European research project, which demonstrates the applications of advanced air quality service tools in urban Europe to improve the assessment of air quality policies, including a better evaluation of health effects. In this context, this study aims to gather and evaluate available NH_3 data from urban areas in five EU countries. The major objective includes comparing NH_3 concentrations among these regions and different environments (urban, traffic, rural, industrial), identifying NH_3 hotspots, contrasting them with background NH_3 concentrations and with levels reported elsewhere, and studying the temporal trends of NH_3 concentrations within the research area across various types of locations. The goal of this study is to understand the variability and origin of NH_3 in urban areas and assess the impact of non-agricultural sources on NH_3 ambient concentrations. The outputs of these analyses contribute to a better understanding of the phenomenology of NH_3 in urban Europe. The outcomes of this study are likely to provide valuable insights of urban NH_3, aiding in the development of effective strategies to address air quality challenges in European cities.

2. Methodology

2.1. Cities and sites providing NH_3 data

This study incorporates data collected from various locations across Europe, including Finland (1 site), France (15 sites), Italy (12 sites), Spain (36 sites), and the UK (5 sites). The dataset comprises 5 industrial (IND) sites, 12 traffic (TR) sites, 25 urban background (UB) sites, 12 suburban background (SUB) sites, and 15 regional background (RB) sites (Fig. 1 and Table S1). These data were provided by regional air quality monitoring networks and research supersites in the framework of RI-URBANS. Specifically, industrial sites (IND) are situated in industrial areas or close to significant industrial sources. These sites are designated for studying the impact of industrial activities on pollutant concentrations and capturing the contributions of industrial emissions to the surrounding environment. Traffic sites (TR) are located in traffic-dense areas, proximate to major traffic routes or vehicle emission sources, aiming to investigate the influence of traffic activities on pollutant concentrations. Apart from IND and TR sites, this study identifies background sites, which are classified into three categories: urban background (UB), suburban background (SUB), and regional background (RB) sites. UB sites are positioned within cities but away from major pollution sources, recording pollutant levels under typical urban background conditions. SUB sites are situated on the outskirts or in suburban areas, distant from the city center, designed to capture general background conditions in the vicinity of urban areas. RB sites are positioned within larger regions, far from urban influences, providing regional background pollution levels unaffected by urban influences, but in some cases highly affected by farming and agricultural sources. While the primary focus of this study is on UB, TR, and SUB sites, the inclusion of IND and RB sites serves to provide additional context for the interpretations. The abbreviated names of these sites are as follows:

- Industrial sites: Lorca (LOR), Sannazzaro de' Burgondi (PAV), Puertollano (PUE), A Coruña (COR), and Castellón (CS).
- Traffic sites: Barcelona (BCN), Bordeaux Gautier (BOR), Valladolid (EMB), Erandio (ERA), Madrid (MAD), Málaga (MAL), Murcia (MUR), Paris (PAR), Poitiers-le Nain (POI), Sevilla (SEV), and Valencia (VLC_1,2).
- Urban background sites: Valladolid (ARG, CAN, LAG, OBR, PDR), BCN_1, 2, 3, Bergamo (BER), Birmingham (BIR), Cremona (CRE), Gonfreville l'Orcher (GOR), Helsinki (HEL), London (LND), Málaga (MAL), Manchester (MAN), Manlleu (MANL), Milano (MIL), Niort Venise (NIO), Paris (PAR), Pavia (PAV), Petit Queuvilly (PQUE), Quai de Paris (QDP), Reims (REI), and Strasbourg (STR).
- Suburban background sites: Colico (COL), CRE, Valladolid (JAR), Málaga (MAL), Milano (MIL), Monza (MON), PAR_1, 2, 3, Poses (POSE), and Vic (VIC_1, 2).
- Regional background sites: Auchencorth Moss (ACTH), Barcarrota (BAR), Bujaraloz (BUJ), Campisábalos (CAM), Chilbolton (CHIL), CRE_1, 2, Lo-bertonico (LO), Montsec (MSC), Montseny (MSY), Niembro (NIE), Schivenoglia (SCH), San Pablo de los Montes (SPM), Els Torms (TOR), and Víznar (VIZ).

For the evaluation of the interannual and seasonal variations of NH_3, the sites with data spanning over five years were selected, including 3 IND, 5 TR, 5 UB, 2 SUB, and 11 RB (Table 1). Additionally, by combining information from remote sensing (Van Damme et al., 2018), and publicly accessible inventories (IFDC, 2016; GSTC, 2018), certain sites have been pinpointed as belonging to farming/agricultural NH_3 hotspots (FAHs) (Fig. S1). These include also the RB sites with an arbitrary average concentration > 1.5 μg/m^3, named RBCH, that accounts for RB sites close to hotspots and only for the farming hotspot regions. These are PAV_IND_UB, LOR_IND_SUB, MUR_TR_SUB, BER_UB, CRE_UB, MANL_UB, MIL_UB, PAV_UB, CRE_SUB, MIL_SUB, MON_SUB, VIC_SUB1, VIC_SUB2, BUJ_RBCH, CHIL_RBCH, CRE_RBCH1, CRE_RBCH2, LO_RBCH, MSC_RBCH, SCH_RBCH, SPM_RBCH, and TOR_RBCH.

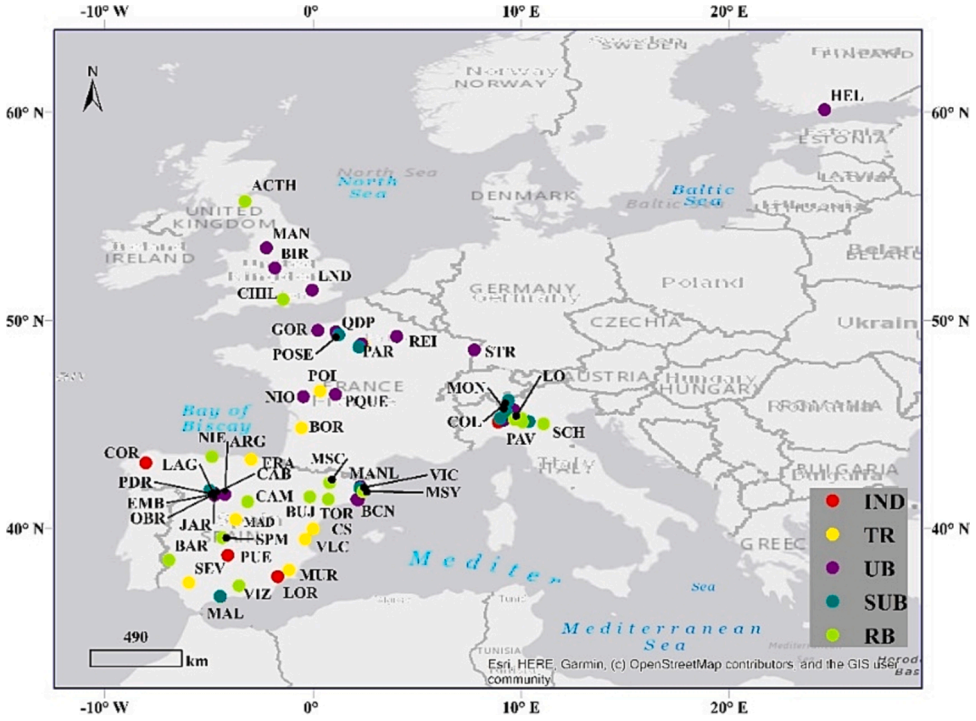

Fig. 1. Location of the sites supplying data on NH_3 concentrations for the present study and the type of station. IND, industry (red point); TR, Traffic (yellow point); UB, Urban background (violet point); SUB, Suburban background (green point); RB, Regional background (light green point). (For interpretation of the references to colour in this figure legend, the reader is referred to the web version of this article.)

Table 1
Instruments used to measure NH_3 in the different stations. UB, Urban Background; TR, Traffic; SUB, Suburban Background; RB, Regional Background. RBCH, Regional Background Closed Hotspot.

Location	Start date	End date	Resolution	Method	Location	Start date	End date	Resolution	Method
LOR_IND_UB	2018/4/16	2023/7/25	Hourly	Chemiluminescence	PAR_UB	2020/3/10	2021/12/31	Hourly	Spectroscopic CRDS
PAV_IND_UB	2013/10/16	2022/6/30	Hourly	Chemiluminescence	PAV_UB	2012/1/1	2022/6/30	Hourly	Chemiluminescence
PUE_IND_UB	2007/1/1	2023/7/25	Hourly	Chemiluminescence	PDR_UB	2021/9/21	2022/12/31	Hourly	Chemiluminescence
COR_IND_SUB	2020/5/11	2022/12/12	Daily	Dosimeters	PQUE_UB	2016/9/1	2019/3/1	Hourly	Spectroscopic CRDS
CS_IND_SUB	2022/1/1	2023/7/1	Daily	Chemiluminescence	QDP_UB	2020/3/13	2020/7/8	Hourly	Spectroscopic CRDS
BCN_TR	2013/11/20	2018/6/29	Daily	Dosimeters	REI_UB	2016/1/1	2023/1/1	Hourly	Spectroscopic CRDS
BOR_TR	2022/2/10	2022/12/29	2 weeks	Dosimeters	STR_UB	2019/1/1	2022/12/31	Hourly	Spectroscopic CRDS
EMB_TR	2023/1/10	2023/4/30	Hourly	Chemiluminescence	COL_SUB	2013/12/3	2022/6/30	Hourly	Chemiluminescence
ERA_TR	2014/1/1	2022/3/11	Hourly	Chemiluminescence	CRE_SUB	2013/7/4	2018/8/1	Hourly	Chemiluminescence
MAD_TR	2012/6/19	2012/7/17	2 weeks	Dosimeters	JAR_SUB	2020/6/13	2021/9/16	Hourly	Chemiluminescence
MAL_TR	2014/1/13	2021/12/20	3 weeks	GC–MS	MAL_SUB	2011/5/16	2013/12/23	2 weeks	GC–MS
MUR_TR_SUB	2023/4/1	2023/7/14	Daily	Chemiluminescence	MIL_SUB	2021/7/12	2021/11/12	Hourly	Chemiluminescence
PAR_TR	2020/11/10	2021/12/31	Hourly	Spectroscopic CRDS	MON_SUB	2013/2/8	2019/7/9	Hourly	Chemiluminescence
POI_TR	2022/2/22	2022/12/27	2 weeks	Dosimeters	PAR_SUB1	2017/5/22	2021/6/21	5 min	AiRRmonia
SEV_TR	2011/5/16	2022/12/5	2 weeks	GC–MS	PAR_SUB2	2012/3/12	2013/5/18	Hourly	AiRRmonia
VLC_TR1	2015/4/28	2023/3/1	Hourly	Chemiluminescence	PAR_SUB3	2018/1/22	2018/4/17	Weekly	Dosimeters
VLC_TR2	2021/7/27	2021/12/31	Hourly	Chemiluminescence	POSE_SUB	2023/6/23	2023/8/29	Hourly	Spectroscopic CRDS
ARG_UB	2019/10/14	2020/4/21	Hourly	Chemiluminescence	VIC_SUB1	2018/6/27	2018/7/29	10 min	Chemiluminescence
BCN_UB1	2011/2/14	2022/2/7	Weekly	Dosimeters	VIC_SUB2	2015/7/10	2015/7/17	1 min	Chemiluminescence
BCN_UB2	2011/6/15	2011/7/29	Minutes	AiRRmonia	ACTH_RB	2018/1/1	2021/1/2	Hourly	MARGA
BCN_UB3	2011/6/15	2011/6/30	Minutes	AiRRmonia	BAR_RB	2012/9/12	2013/12/29	Weekly	Dosimeters
BER_UB	2021/2/18	2022/6/30	Hourly	Chemiluminescence	BUJ_RBCH	2020/7/9	2023/5/16	2 weeks	Dosimeters
BIR_UB	2019/1/4	2021/1/1	Hourly	Spectroscopic HFOC	CAM_RB	2004/8/2	2022/12/26	Weekly	Dosimeters
CAB_UB	2018/12/31	2019/2/11	Hourly	Chemiluminescence	CHIL_RBCH	2018/1/1	2021/1/2	Hourly	MARGA
CRE_UB	2011/2/15	2022/6/30	Hourly	Chemiluminescence	CRE_RBCH1	2011/10/1	2021/12/31	Daily	Chemiluminescence
GOR_UB	2020/7/9	2023/8/22	Hourly	Spectroscopic CRDS	CRE_RBCH2	2007/1/1	2021/12/31	Hourly	Chemiluminescence
HEL_UB	2009/11/1	2010/5/25	Hourly	MARGA	LO_RBCH	2009/3/3	2021/12/31	Daily	Chemiluminescence
LAG_UB	2019/5/8	2019/10/6	Hourly	Chemiluminescence	MSC_RBCH	2011/2/15	2021/5/5	Monthly	Dosimeters
LND_UB	2019/1/1	2020/11/22	Hourly	Spectroscopic HFOC	MSY_RB	2011/2/18	2022/1/14	Monthly	Dosimeters
MAL_UB	2011/5/16	2011/12/31	2 weeks	GC–MS	NIE_RB	2004/8/2	2022/12/26	Weekly	Dosimeters
MAN_UB	2018/1/1	2020/12/31	Hourly	Spectroscopic HFOC	SCH_RBCH	2013/2/15	2022/6/30	Hourly	Chemiluminescence
MANL_UB	2021/1/1	2023/1/1	2 weeks	Chemiluminescence	SPM_RBCH	2012/6/5	2022/12/26	Weekly	Dosimeters
MIL_UB	2007/6/15	2021/12/31	Hourly	Chemiluminescence	TOR_RBCH	2012/8/20	2022/12/26	Weekly	Dosimeters
NIO_UB	2022/1/25	2022/12/27	2 weeks	Dosimeters	VIZ_RB	2012/8/27	2022/12/12	Weekly	Dosimeters
OBR_UB	2019/2/12	2019/5/6	Hourly	Chemiluminescence					

2.2. Measurements

Measurements of NH_3 were conducted at the different stations using a wide variety of approaches (Table 1). The instruments used include: (i) active denuders and passive samplers or dosimeters that trap NH_3 during 1–2 weeks and after extraction the concentrations are determined by different analytical tools (Twigg et al., 2022); (ii) online measurements with a high time resolution, such as chemiluminescence equipped with an NH_3 converter (Sharma et al., 2010), gas chromatography-mass spectrometry (GC–MS), Optical CRDS (Cavity Ring-Down Spectroscopy, such as PICARRO G2103 (Winkler and Adamsen, 2017), Optical HFOC (High-Finesse Optical Cavity, Los Gatos DTL-100 (Baer et al., 2002)); and (iii) near-real-time high time resolution measurements, such as the AiRRmonia analyzer (further development of the AMANDA technique, equipped with an annular denuder sampling with on-line analyses) (Norman et al., 2009), and MARGA (Measuring AeRosols and GAses), an online ion chromatography-based system that measures water-soluble gases and aerosols at an hourly temporal resolution (Makkonen et al., 2012; Rumsey et al., 2014; Twigg et al., 2015). Specifically, among the monitoring stations, 30 out of 69 utilized Chemiluminescence with a detection limit of 0.7 $\mu g/m^3$, followed by Dosimeters (17/69) with a detection limit of 0.01 $\mu g/m^3$, and Optical (HFOC/CRDS) methods (11/69) with a detection limit of 0.02 $\mu g/m^3$. Additionally, 4 out of 69 stations employed GC–MS (detection limit: 0.01 $\mu g/m^3$), 4 out of 69 used AiRRmonia (detection limit:0.05 $\mu g/m^3$), and 3 out of 69 utilized MARGA (detection limit 0.05 $\mu g/m^3$ or 0.72 ppb with an overall uncertainty of 5 %) (Makkonen et al., 2012).

2.3. Data treatment

NH_3 concentrations are reported as average concentration (AVE) ± standard deviation (STD). Due to varying resolutions among monitoring sites, for a more robust comparison of concentration differences across sites, this study initially normalized all data. Specifically, we adjusted the data resolution for all sites to a weekly basis and conducted comparisons based on this standardized framework. This step was taken to ensure consistent and meaningful comparisons across different time intervals. Statistically significant differences in NH_3 concentrations at different monitoring sites and during different seasons were studied using the Kruskal-Wallis ANOVA on ranks (Kruskal and Wallis, 1952) and Duncan's Multiple Range Test (Duncan, 1955), which were performed using the SPSS Software (IBM SPSS Statistics 25, Chicago, IL, USA). Subsequently, to elucidate the interannual trend in NH_3 concentration, this study utilized the Mann-Kendall (MK) test (Mann, 1945; Kendall, 1948; Gilbert, 1987) with the Theil-Sen estimator (Salmi et al., 2002). Sen's method was applied to estimate the trend's slope. The interannual trend in NH_3 concentration, whether increasing or decreasing, is clarified by assessing the significance level and the Sen's slope value. Data treatment and statistical analysis were carried out using the R statistical software (v4.1.3) and the Openair package (Carslaw and Ropkins, 2012).

The individual slopes estimated as a percentage change per year with 95 % CI (confidence interval), extracted from the Mann Kendall test, were summarized by *meta*-analysis using the "meta" R package version 6.5–0 (Balduzzi et al., 2019). The analysis is based on random-effects model due to the heterogeneity of the data among the included sites, which involves variability in the effects sizes (Chen and Peace, 2013). The mean effect was calculated for each class of site individually (Industry, urban-traffic, urban-background, suburban-background and regional-background) as well as globally to provide a comprehensive overview of the results.

3. Result and discussion

3.1. Status of NH_3 data availability and concentrations in urban Europe

Fig. 2a visually presents both the long-term and short-term average values of NH_3 at each monitoring site, emphasizing significant difference in NH_3 concentrations across the five European countries. On average, mean NH_3 concentrations considering all dataets reached 8.0 ± 8.9 μg/m^3, and ranged from 0.2 to 54.4 μg/m^3. From all these, 48/69 sites significantly exceeded the critical threshold of 1 μg/m^3 set for NH_3 to protect ecosystems and the 3 μg/m^3 threshold for other vegetation (UNECE, 2007; Cape et al., 2009). Similarly, individuals residing in areas with elevated NH_3 concentrations face corresponding higher health risks (Wyer et al., 2022).

As explained in the methodology, to facilitate a better comparison of NH_3 concentrations across different environment types, an analysis excluding FAH sites was performed. After excluding these FAHs, the average NH_3 concentration reached 3.2 ± 1.8 μg/m^3, whereas for the FAHs the mean concentration was 4-fold higher, 14.1 ± 10.8 μg/m^3. Northern Italy is the largest FAH in Europe (Van Damme et al., 2018) and the average for these the 12 sites reached 16.9 ± 14.1 μg/m^3. Excluding the FAHs, the overall annual mean concentrations reached 4.7 ± 3.2 and 4.5 ± 1.0 μg/m^3, respectively at IND and TR sites > UB (3.3 ± 1.5 μg/m^3) > SUB (2.7 ± 1.3 μg/m^3) > RB (1.0 ± 0.3 μg/m^3) (Fig. 2b). Due to the rapid dissipation of NH_3 near-source, aerosol uptake and dry deposition fluxes, variations in NH_3 its concentration are more highly influenced by nearby-source emissions (Ferm, 1998). As a result, NH_3 concentrations were higher at TR sites compared to UB sites, owing probably to relevant NH_3 traffic emissions, but still much lower than those of equivalent FAH sites. Similarly, Wang et al. (2022) revealed that traffic sources accounted for 8 % of the overall NH_3 levels in urban Beijing, with the most significant seasonal impact occurring during winter at 22 %. Additionally, UB sites may experience larger concentrations due to city's waste treatment and sewage systems that could also

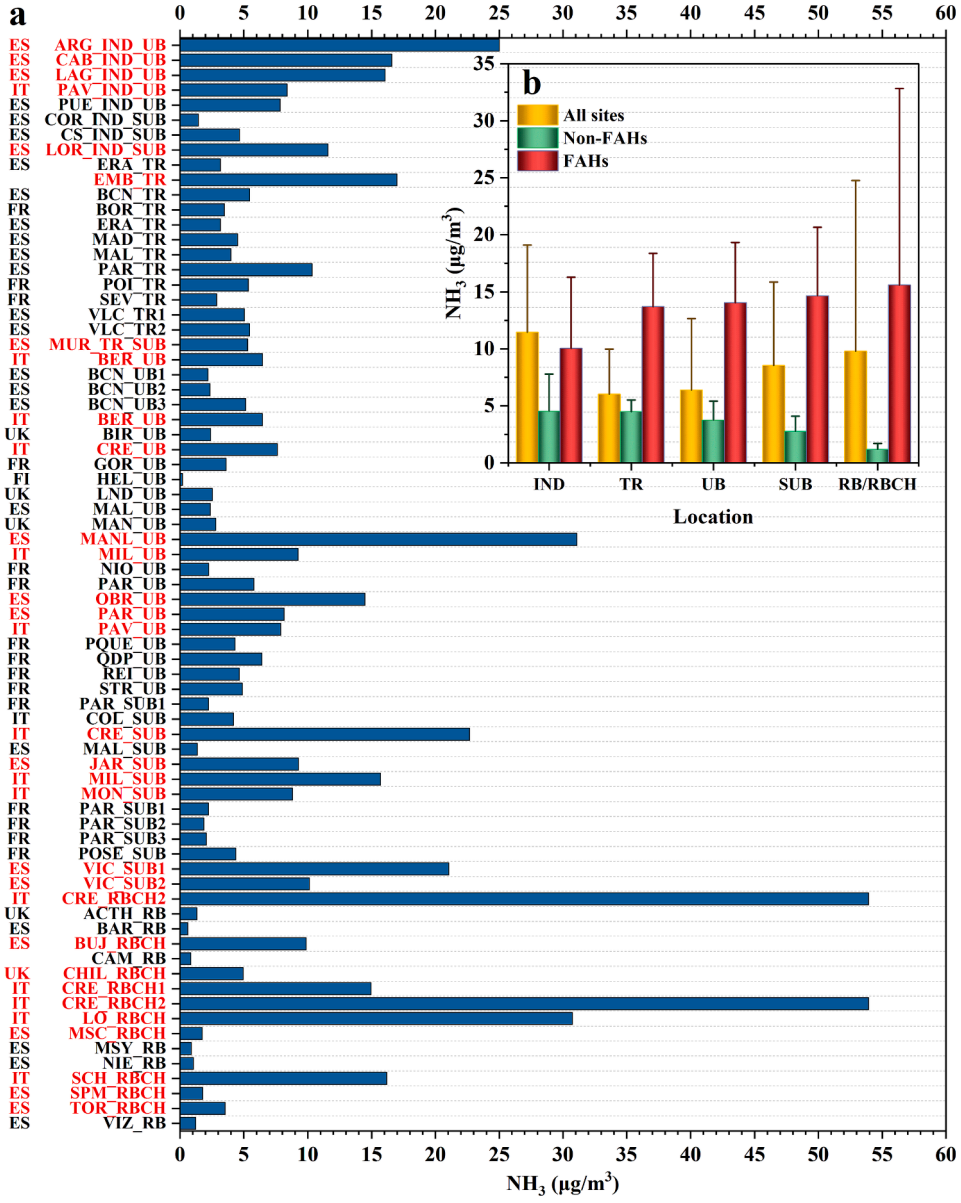

Fig. 2. (a) Average NH_3 concentrations of the 69 European datasets compiled in this study (red, farming/agricultural hotspots (FAHs)). (b) Idem but for different environments: Industry, IND; traffic, TR; urban background, UB; and suburban background, SUB; RB, regional background. RBCH, regional background site close to farming/agricultural sources in FAHs. Error bars indicates one standard deviation. (For interpretation of the references to colour in this figure legend, the reader is referred to the web version of this article.)

significantly impact urban NH_3 levels (Pandolfi et al., 2012; Reche et al., 2012), and increase (together with those from traffic) UB levels compared with the RB ones from non-FAHs. Therefore, in non-FAHs, industrial, traffic and other urban sources (*e.g.*, fugitive emissions from city waste treatment and sewage systems) are the main contributors to NH_3 ambient concentrations at UB sites. However, some of these emissions may be underestimated in the EU-27 emission inventory. Therefore, it is crucial to enhance monitoring of urban NH_3 sources and improve emission inventories to more accurately assess the potential impact of urban NH_3 on the environment and health. This will provide relevant information for the development of appropriate environmental policies and measures, such as the implementation of technologies aimed at diminishing NH_3 emissions from industrial and traffic sources and adequate management of urban wastes and sewage systems.

However, when only FAHs were considered (Fig. 2b), an opposite contrasting NH_3 concentration trend was observed across the various environments: SUB and RBCH (14.7 ± 6.0 and 15.6 ± 17.2 $\mu g/m^3$, respectively) > UB (14.0 ± 5.3 $\mu g/m^3$) > TR (13.7 ± 3.6 $\mu g/m^3$) > IND (10.0 ± 2.3 $\mu g/m^3$). Therefore, it is evident that SUB and RBCH have the largest concentration (e.g., CRE_SUB/RBCH, LO_RBCH, and SCH_RBCH). This probably due to the closer proximity to the nearby agriculture and livestock sources (Misselbrook et al., 2004; Pinho et al., 2009), compared to the more UB- and TR- oriented FAH sites. This increase can be very high, as shown by the remote sensing data (Fig. S1), and many of the RBCH are located very close to NH_3 FAH sources. Additionally, the lower levels of NO_X available to react with NH_3 in these RBCH sites might lead to a lower NH_3 consumption to generate secondary PM (Reche et al., 2015). Conversely, in urban areas, particularly in traffic zones, there is a higher availability of NO_X, which might reduce NH_3 concentrations.

For non-FAHs UB sites, Paris (PAR_UB) reached the highest NH_3 concentration (5.8 ± 1.9 $\mu g/m^3$), followed by Strasbourg (STR_UB, 4.9 ± 1.6 $\mu g/m^3$) and Reims (REI_UB, 4.7 ± 3.2 $\mu g/m^3$), all in northern France. The UB sites with lowest mean concentrations were Niort (NIO_UB, France), with a mean of 2.3 ± 1.1 $\mu g/m^3$, and Helsinki, (HEL_UB), with 0.2 ± 0.3 $\mu g/m^3$ (Fig. 2a). Considering only non-FAHs, very similar UB concentrations were recorded, data from Helsinki and Paris are excluded. Some northern Italian and Spanish regions (in Southern Europe) observed the highest UB concentrations because these are located in FAH regions, based on (Van Damme et al., 2018).

Average NH_3 concentrations at UB-FAH sites reached 14.0 ± 5.3 $\mu g/m^3$, 4-fold higher than that of the UB-non-FAH sites, 3.3 ± 1.5 $\mu g/m^3$. Comparing with other reported worldwide concentrations, these might be characterized as intermediate (Table S2). Specifically, these are higher than those from UB sites in North America (1.1–1.7 $\mu g/m^3$, in Toronto, (Yao and Zhang, 2016), and 2.0–2.3 $\mu g/m^3$, in Rochester and Queens NY, (Zhou et al., 2019)), and similar (in the case of the non-FAHs UB, but lower in the case of the FAHs ones) to those of Chinese cities of Nanjing, Shanghai (5.5–6.7 $\mu g/m^3$, (Chang et al., 2016), Beijing (Zhang et al., 2021), to Seoul (Singh et al., 2021), and to Delhi in India (Saraswati et al., 2018) (13.5–18.2 $\mu g/m^3$). Therefore, in urban areas in Europe, special attention should be given to industrial, traffic and other urban sources (such as waste management), as the major contributors to urban NH_3 emissions. However, agricultural and farming emissions are the main NH_3 contributors to the concentrations recorded at UB-FAH sites, leading to mean concentrations 4-fold higher than that of the UB-non-FAH sites.

3.2. Temporal trends in NH_3 concentrations

3.2.1. Inter-annual trend

The official NH_3 emissions inventories (EMEP-CEIP, 2023) of the five countries evidenced that in the last decade Finland and Italy decreased emissions, but not Spain and the UK (Fig. S2), which increased slightly. The increases and decreases in each case were driven by estimated changes in agricultural and farming emissions. Estimated emissions from waste management were constant or increased slightly, while those from industry and road transport decreased.

The analysis of inter-annual trends of NH_3 concentrations were only implemented for those datasets with over 5 years of data availability. From the 69 datasets, only 26 met this criterion, 13 of which were in FAHs.

The evaluation of temporal trends reveals that during the study period, over half (18 out of 26) of the monitoring sites exhibited statistically significant monotonic trends at the 95 % confidence level (Fig. 3). Some sites, particularly SUB sites from northern Italy and France (*i.e.,* COL_SUB, CRE_SUB, MIL_SUB, MON_SUB, and PAR_SUB), remained relatively stable. This trend could be related to a combination of the ones of urban NH_3 and regional farming/agricultural emissions, yielding constant concentrations. Among IND sites, PUE_IND_UB showed a significant annual increase, with a yearly Sen's slope of 11 [6–22] %/yr in 2007–2022). The principal contributor to this heightened pollution may be the emissions of a petrochemical hub located approximately 5–6 km southeast of the city. This hub encompasses various industries including a refinery, several chemical plants, and two power plants, collectively exerting a significant impact on air quality in the area (Saiz-Lopez et al., 2009).On the other hand, trends at the other industrial sites - LOR_IND_SUB and PAV_IND_UB - remained relatively stable.

The sites ERA_TR, VLC_TR1, and REI_UB (in non-FAHs), MIL_UB, and PAV_UB (in FAHs) experienced significant declines ($p < 0.05$) throughout the years. This reduction may be attributable to the enforcement of traffic control measures, transportation system upgrades, and other initiatives aimed at mitigating the impact of tailpipe and other urban emissions (waste management for example), but in some cases also to decrease of emissions from agriculture/farming. For instance, important traffic reductions have been attained in Milano and Valencia due to the different urban measures implemented (congestion tax, low emission zones, among others in the first case, and urban street changes in the second (UAR, 2023)). However, the heightened traffic density, and the effect of the NH3 slip from SCR-equipped diesel vehicles in both Málaga (Grindlay and Martínez-Hornos, 2017) and Sevilla (Florido et al., 2015), might have resulted in the significant upward trends for MAL_TR and SEV_TR ($p < 0.01$). For Barcelona, NH_3 concentrations at the BCN_TR site (measurements finished in 2018) remained constant throughout the years, but the BCN_UB site showed a significant upward trend (Sen's slope of 10 [6,15] %/yr, $p < 0.01$), suggesting that traffic is not the only source of urban NH_3 in Barcelona, although NH_3 concentrations were higher at the TR site than at the UB one in this city. Thus, other sources such as the city waste management might be a relevant source of urban NH_3 in the city (Pandolfi et al., 2012; Reche et al., 2012). Three RB sites in Spain, CAM_RB, MSY_RB, and VIZ_RB had constant averages throughout the study period, while CRE_RBCH1, LO_RBCH, MSC_RBCH, SCH_RBCH, SPM_RBCH, and TOR_RBCH (in FAHs in Italy and Spain) followed a significant increase, pointing to a probable increase in agricultural/farming emissions in these study areas during the corresponding period. This was also reported by Reche et al. (2022) for MSC_RBCH. Conversely, CRE_RBCH2 and NIE_RB showed significant decreases throughout the years. On the whole, the average annual incremental in NH_3 concentrations across all sites increased at a rate of 1.28 [-0.64, 3.19] %/yr, and at 1.05 [-1.94, 4.03] %/yr and 1.56 [-0.90, 4.03] %/yr for non-FAH and FAH sites, respectively, thus increasing in all cases but without statistical significance (Fig. S3).

Three out of the 7 UB and TR sites in non-FAHs observed a significant decreasing trend (ERA_TR, VLC_TR, and REI_UB, Fig. 4a) as it does in 2/3 of the UB sites in FAHs areas (MIL-UB and PAV_UB trend, Fig. 4b). Only 3/7 UB and TR sites in non-FAHs follow a statistically significant increasing trend (BCN_UB, SEV_TR, and MAL_TR). Thus, 50 % of the UB and TR sites followed a downward trend, while a 30 % observed an upward trend.

The *meta*-analysis for the non-FAH sites revealed a slight non-

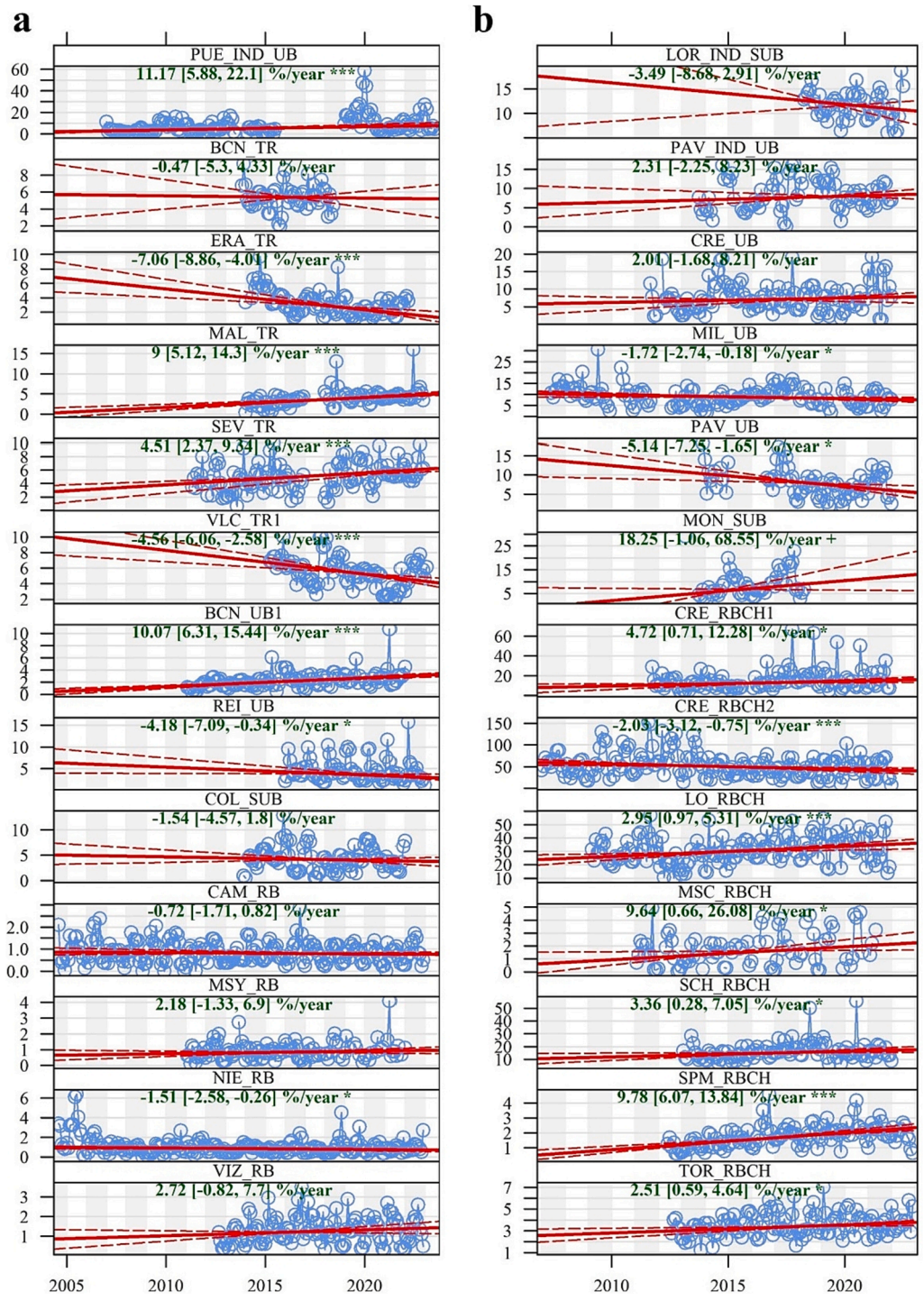

Fig. 3. The trends in NH_3 concentrations at the non-FAHs (a) and FAHs (b) sites with time series > 5 years. Sen's slope of long-term period data is indicated in green, expressed as an average annual percent change. $p < 0.001$ = ***, $p < 0.01$ = **, $p < 0.05$ = *and $p < 0.1$ = +; (blank) non statistically significant. (For interpretation of the references to colour in this figure legend, the reader is referred to the web version of this article.)

significant decreasing trend for the RB sites (-0.35[-1.90, 1.19] %/yr), while in the case of the FAHs RBCH sites a statistically significant increasing trend (3.51[0.45, 6.57] %/yr) (Fig. 4), This increasing trend at FAH RBCH sites don't follow the decreasing trend reported in the emission inventories (see above). As stated above, Behera and Sharma (2011), Banzhaf et al. (2013), Fagerli et al. (2021), and Jonson et al. (2022) attributed the NH_3 increasing trends of RB NH_3 to the progressive decrease of NH_3 consumption to generate $(NH_4)_2SO_4$ and NH_4NO_3 due to the marked abatement of SO_2 and NO_x emissions. In any case the fact that this increasing trend is found only at RBCH sites (with very high NH_3 concentrations) and not at the RB ones probably points to an increase of emissions. However, the number of measurement sites is quite small, and they may not be representative of the entire country, so comparison with national emissions trends may be misleading.

3.2.2. *Seasonal variation*

The seasonal NH_3 patterns (spring: March to May, summer: June to August, autumn: September to November, and winter: December to

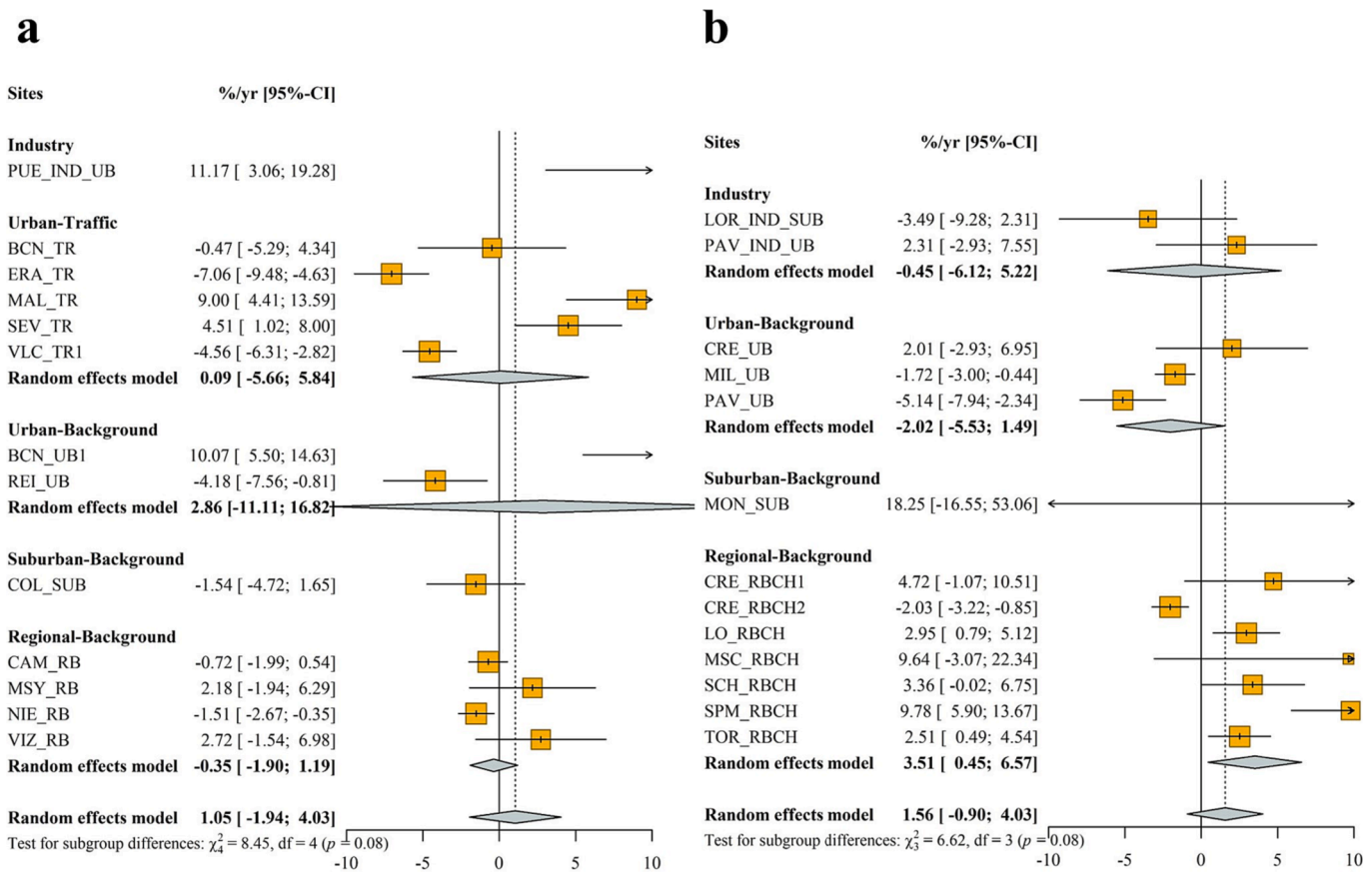

Fig. 4. Meta-analysis results for the NH_3 trends at non-FAHs (a) and FAHs (b). Values are given and represented for slope [95 % CI] in %/yr.

February (Lloyd Hughes and Saunders, 2002; Liu et al., 2022) were evaluated for total sites, non-FAHs, and FAHs using ANOVA on ranks with Dunn's method (Fig. 5 and S4). Significant seasonal differences ($p < 0.01$) in NH_3 concentrations were observed across the monitoring sites, influenced by changes in emissions, chemical interactions, and the influence of meteorology on partitioning between the main inorganic gases and aerosol species. These seasonal variations highlight the dynamic relationships between each season and NH_3 concentrations (Tang et al., 2021).

At IND sites, NH_3 concentrations were higher in summer and autumn compared to spring and winter for LOR_IND_SUB and PAV_IND_UB (in FAHs from Spain and Italy) (Fig. S4). These sites are affected by emissions from agriculture and farming but also by nearby leather manufacturing factories (Gabarrón et al., 2017) and oil refineries (Pasini, 2022). PUE_IND_UB showed higher Winter NH_3 concentrations, and less variation in the other three seasons, possibly due to the local industrial emissions and the intense thermal winter inversion in an inner closed basin (Saiz-Lopez et al., 2009), which favors accumulation of local pollutants compared in the warmer season. Therefore, it is recommended to regulate emissions from these industrial facilities such as leather manufacturing factories and oil refineries, and implement advanced emission control technologies. At TR sites, Autumn and Winter NH_3 concentrations were significantly higher, probably due to lower dispersion conditions and higher NH_3 emissions from vehicular cold starts near traffic sites (Farren et al., 2021). It has been reported that NH_3 cold-start emissions from gasoline vehicles were up to 2 orders of magnitude higher than entire duration of road trips (Suarez-Bertoa et al., 2017).This possibility highlights the importance of considering the implementation of NH_3 emissions limits for all times of vehicles (as requested in the forthcoming EURO 7/VII standards), especially because such limits currently apply only to heavy-duty vehicles (EURO VI) in the EU. Promoting cleaner and low NH_3-emission vehicles for traffic, along with optimizing traffic management measures, becomes imperative in addressing these findings.

At the UB sites, the seasonal heterogeneity was primarily driven by the CRE_UB (a FAH site), showing lower concentrations in winter compared to the other seasons ($p < 0.01$) (Fig. S4), linked to the influence of temperature and rainfall on emissions, deposition, and gas–aerosol-phase equilibrium (Tang et al., 2021). In contrast, the remaining three UB sites (BCN_UB1, MIL_UB, and PAR_UB) did not display significant fluctuations in NH_3 concentrations across seasons.

At SUB sites, seasonal NH_3 patterns were less marked with only significant differences between summer and autumn ($p < 0.01$) (Fig. 5). This difference was mainly due to seasonal variations in NH_3 concentrations at different suburban background points. Specifically, COL_SUB recorded higher NH_3 in spring and winter compared to summer and autumn, reflecting an important contribution from mineral fertilizer and manure application in spring (Paulot et al., 2014).While MON_SUB showed the highest NH_3 concentrations in autumn and the lowest in summer, this phenomenon may be due to meteorological conditions such as lower wind speeds in autumn and a stable atmosphere that are not conducive to air pollution diffusion (Silvaggio et al., 2020).

At RB/RBCH sites, most monitoring sites observed the highest NH_3 concentrations in summer and autumn (Fig. 5), as a result of spreading of manure and livestock going back indoors and application of fertilizers (Sutton et al., 2022; Hellsten et al., 2007, Marais et al., 2021), and higher temperatures favoring the occurrence of NH_3 against NH_4NO_3..

NH_3 concentrations peaked in spring at UB non-FAHs sites (Fig. 5b), compared to the little seasonal variation observed at UB-FAH sites, with similar concentrations in spring, summer, and autumn, and lower in winter. This difference suggests that seasonal fluctuations in urban areas are affected by emissions from the surrounding areas, e.g., increasing

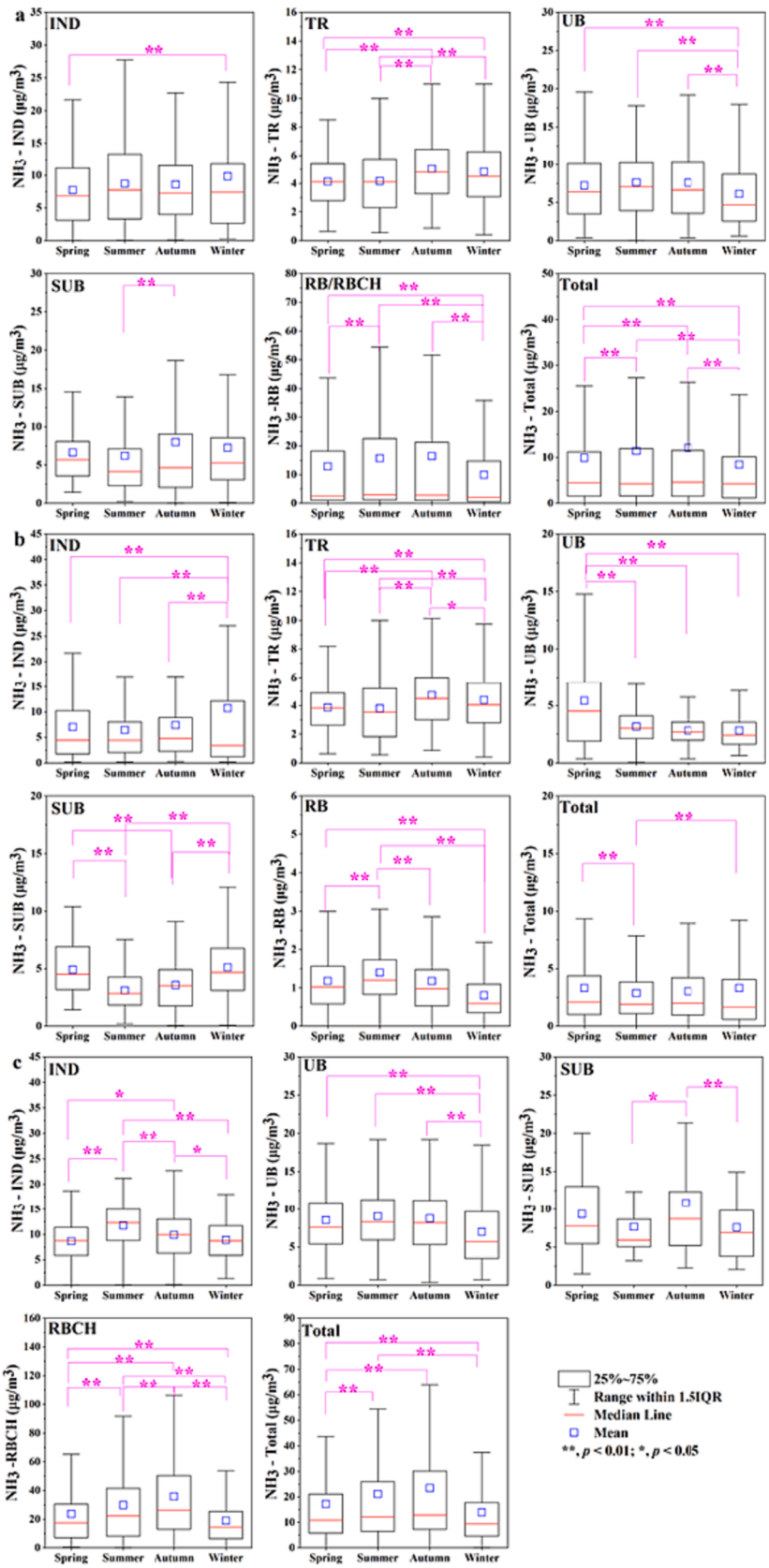

Fig. 5. Seasonal variability in NH_3 concentrations across different environments (industry, IND; traffic, TR; urban background, UB; and suburban background, SUB) and total monitoring sites. (a, including all monitoring sites, b, non-FAHs, c, FAHs).

soil emission in spring associated with fertilization activities. Therefore, these research findings underscore the influence of pollution sources and meteorological factors on the seasonal variations in urban NH_3 concentrations. We recommend strengthening fertilizer and manure management practices in agriculture to reduce NH_3 emissions. In literature, results also show remarkable variability, for instance, in a study in northeastern Colorado, USA, NH_3 concentrations peaked in summer, nearly doubling those observed in spring and autumn (Day et al., 2012). Conversely, higher NH_3 concentrations in winter compared to summer have been reported for certain regions of Japan (Nguyen et al., 2021).

Interpretation of seasonal trends is complex for NH_3. The emissions from agriculture are likely to increase in hotter months, when NH_4^+ salt dissociation is also favored. However, this is likely to be counteracted by an increased mixing depth, and the net outcome is uncertain. Another key factor is likely to be the seasonality of agricultural practices, such as application of fertilizers and disposal of animal waste slurry on the land. This will vary across Europe, with the different climates and crops existing across the continent, so no common behavior is expected.

3.2.3. Diel variation

Only sites with hourly resolution NH_3 data in non-FAHs were considered (PUE_IND_UB, EAR_TR, PAR_TR, VLC_TR1, BIR_UB, GOR_UB, LND_UB, PAR_UB, PQUE_UB, REI_UB, and STR_UB) (Fig. 6). NH_3 concentrations exhibited a single diel peak varying in intensity and amplitude, and time of the maxima. Only, LND_UB slightly peaked at the morning traffic rush hour·NH_3 at PUE_IND_UB sharply peaked at 10 h am and, the lowest hourly NH_3 concentration represented the highest at the other sites. The main reason for the peak at 10 h is the Hewson-type fumigation, where industrial, urban and agricultural sources of NH_3 emitted during the evening and night is accumulated at a given height (bottom of a frequently formed thermal inversion in a closed basin). As convective flows grow in height in the early morning, the thermal inversion is broken and the accumulated NH_3 fumigates surface levels. This area is very peculiar of this basin, and has been described in pervious O_3 studies (Massagué et al., 2023). Other sites such as PAR_TR, PAR_UB, and STRA_UB, peaking with a lower intensity also at 10 h might have a similar origin. However, it has been also found that during the night and early morning condensation of water in the sampling inlets might cause the trapping of NH_4NO_3 aerosols. In the next morning, heating of the inlet by insolation might cause the dissociation of the accumulated NH_4NO_3 into HNO_3 and NH_3, and then typically causing a morning artifact peak that frequently takes place around 9–10 h (Norman et al., 2009; Vaittinen et al., 2018; Twigg et al., 2022). Most of the remaining sites have a variation characterized by a progressive a smooth hump with maxima between 12 and 16 h. One potential explanation for this pattern may be the thermodynamic balance of NH_4NO_3, which tends to dissociate into NH_3 and HNO_3 as temperatures increase (Behera et al., 2013; Wu et al., 2023). Löflund et al. (2002) emphasized a robust association between urban traffic density and NH_3 levels. They identified a linear correlation with an R^2 value of approximately 0.96 when plotting NH_3 concentration against traffic density. This suggests that traffic significantly influences NH_3 concentration in urban settings. However, such a correlation was not observed in the majority of the sites studied here, as mainly reflected by the inconsistent trends between NH_3 concentration and the probable traffic emission density.

As with seasonal patterns, the diel pattern of NH_3 may be regulated by the interplay between daytime temperatures (causing evaporative emissions from soils, wastes, and ammonium salt dissociation), traffic and industrial activities, and variations of meteorology (wind speed, boundary layer height, etc.). However, influences of sampling artifacts cannot be excluded. This highlights the complexity in the study and comprehension of this pollutant. Meanwhile, our study also can guide the implementation of time-specific mitigation strategies, optimizing resource allocation during high NH_3 concentration periods.

4. Limitations

The metrology of ambient NH_3 measurements is a complex issue. Indeed, on one hand, passive dosimeters are frequently being used, but this protocol is considered an indicative method for other (regulated) pollutants (such as SO_2, O_3, NO_2) with higher uncertainty than the reference method. On the other hand, there are higher time resolution NH_3 analyzers that might have a lower uncertainty but important sampling artifacts have been described (Twigg et al., 2022). One of these is the condensation of water in the inlets, especially during the night, that may trap ammonium nitrate aerosols, and during the next morning with the heating of the inlet by insolation causes drying and dissociation of the trapped/accumulated ammonium nitrate into HNO_3 and NH_3, then causing morning peaks of NH_3 (Norman et al., 2009; Vaittinen et al., 2018; Twigg et al., 2022). Therefore, a significant limitation in this

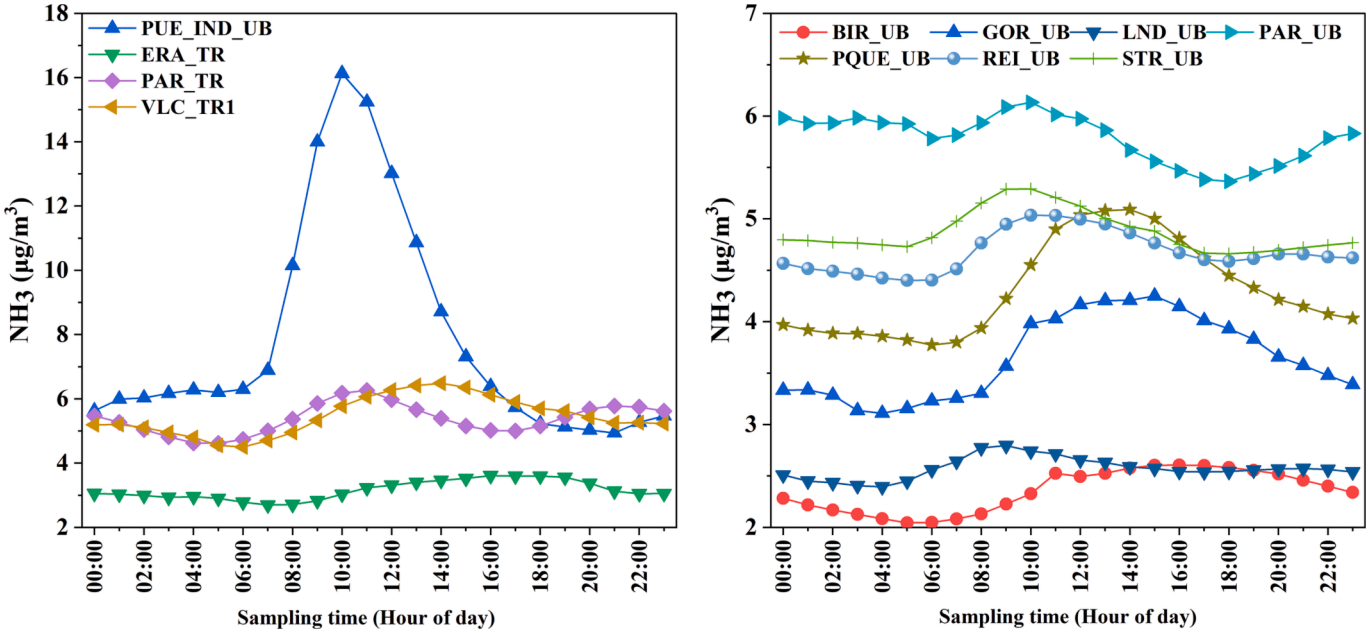

Fig. 6. Diel variations of NH_3 concentrations for 11 out of the 69 studied sites.

study was the monitoring sites utilized a variety of instruments including Chemiluminescence, Dosimeters, GC–MS, Optical CRDS, AiRRmonia, MARGA, GC (TEI 17i), Picarro, and Los Gatos instruments to measure NH_3 concentrations, with an as yet unquantified degree of variability between them (Table 1). There are also inconsistencies in instrument calibration methods, for example, the MARGA instruments used in this study require specialist operators and are labor intensive; however, calibration and quality assurance are accurate and simple, as they use liquid calibrations.

Twigg et al. (2022) conducted a comprehensive comparison of different NH_3 instruments. However, their findings indicated a reduction in the accuracy of NH_3 instruments when concentrations fell below 10 ppb. Furthermore, the performance of repeat instruments of the same model exhibited variations attributable to differences in instrument setup, inlet design, and operational procedures, as reported by Twigg et al. (2022).

Also, the effect of sampling artifacts, described in prior sections, could not be corrected in this study. Despite the datasets being collected by highly specialized research teams, the level of uncertainty in the data is still unknown. Additionally, the number of NH_3 monitoring sites and the duration of monitoring vary among the five countries, along with differences in meteorological conditions across different regions. This introduces a certain degree of error in the comparisons, especially considering the impact of the COVID-19 pandemic from 2020 to 2022, as some sites did not cover this monitoring period. Nonetheless, the study provides valuable insights into the spatiotemporal distribution patterns of NH_3 in urban Europe.

5. Conclusions

In this study, a comprehensive assessment of long and short-term NH_3 concentrations across 69 monitoring sites in five European countries (Finland, France, Italy, Spain, and the UK) is carried out. A wide variety of measurement protocols were implemented with a possible negative impact on the direct comparison of data. Thus, a need for a harmonization of measurements is the first conclusion obtained. Average NH_3 concentrations reached 8.0 ± 8.9 μg/m^3, including all sites, which exceeded the critical thresholds for safeguarding ecosystems. After excluding sites in farming/agricultural hotspots (FAHs), the average NH_3 concentration was 3.2 ± 1.8 μg/m^3, much lower than the one of FAHs sites, 13.6 ± 12.1 μg/m^3. Excluding farming/agricultural hotspots (FAHs), IND and TR sites had the highest concentrations (4.7 ± 3.2 and 4.5 ± 1.0 μg/m^3), followed by UB, SUB, and RB sites (3.3 ± 1.5, 2.7 ± 1.3, and 1.0 ± 0.3 μg/m^3, respectively) indicating that industrial, traffic, and other urban sources were primary contributors to urban NH_3 concentrations outside FAH regions. When referring exclusively to the FAHs, concentrations ranged from 10.0 ± 2.3 to 15.6 ± 17.2 μg/m^3, with the highest concentrations are recorded at RB sites close to the farming/agricultural sources (RBCH sites),), and that, on average there is for these a decreasing NH_3 concentration gradient towards the city as farming/agricultural NH_3 is diluted or reduced.

Italy possessed a significant number of these hotspots (12 sites in total), with the highest average concentration (16.9 ± 14.1 μg/m^3). In terms of temporal variations, about of half of the sites with more than 5 years of monitoring data had, statistically significant monotonic trends. Among them, some urban traffic and background monitoring sites showed a significant decrease in concentrations, which could be attributed to the reduction of emissions from non-agricultural sources as a result of the implementation of measures such as traffic control, upgrading of transportation systems and waste management. The *meta*-analysis of trend for the regional back ground close to agricultural/farming hotspots (RBCH) sites in FAHs showed a statistically significant increase, which is opposite to the reported decrease in emissions from agriculture and farming in a number of official inventories. This increase has also been attributed to the lower consumption of NH_3 to generate $(NH_4)_2SO_4$ and NH_4NO_3 due to the marked decreases in the emissions of SO_2 and NO_X (Fagerli et al., 2021). However, the fact that this increase is only found at RBCH sites from FAHs might also imply and increase in emissions. Thus, it is important that these trends, emissions and atmospheric processes are considered to devise effective NH_3 abating policies (Sutton et al., 2022; Grange et al., 2023).

Regarding seasonal patterns, NH_3 concentrations exhibited variability without consistent trends across the sites, influenced by a combination of emission and meteorological factors. In urban areas, seasonal fluctuations were notably affected by emissions from their surrounding environments. Regarding the diel patterns observed in urban areas, it was observed that NH_3 concentrations were influenced by the interplay between daytime high temperatures (causing evaporative emissions form soils and wastes), traffic and industrial activities, and diurnal variations of meteorology (wind speed, boundary layer height, etc.). Overall, NH_3 concentrations are influenced by both pollution sources, sinks and meteorological factors. Additionally, for non-agricultural pollution sources, especially industrial, city waste management and road traffic sources, measures are needed to reduce NH_3 emissions. Some revision of inventories may be needed to ensure that they are accounting adequately for all sources, such as road traffic. Simultaneously, there is a need to advance unified monitoring technologies to enhance the precision of measuring ammonia concentrations, enabling a more effective tracking and understanding of its dynamic variations.

CRediT authorship contribution statement

Xiansheng Liu: Writing – review & editing, Writing – original draft, Conceptualization. **Rosa Lara:** Software, Formal analysis. **Marvin Dufresne:** Data curation. **Lijie Wu:** Data curation. **Xun Zhang:** Methodology. **Tao Wang:** Methodology. **Marta Monge:** Project administration. **Cristina Reche:** Data curation. **Anna Di Leo:** Data curation. **Guido Lanzani:** Data curation. **Cristina Colombi:** Data curation. **Anna Font:** Data curation. **Annalisa Sheehan:** Data curation. **David C. Green:** Data curation. **Ulla Makkonen:** Data curation. **Stéphane Sauvage:** Data curation. **Thérèse Salameh:** Data curation. **Jean-Eudes Petit:** Data curation. **Mélodie Chatain:** Data curation. **Hugh Coe:** Data curation. **Siqi Hou:** Data curation. **Roy Harrison:** Data curation. **Philip K. Hopke:** Writing – review & editing. **Tuukka Petäjä:** Writing – review & editing. **Andrés Alastuey:** Writing – review & editing. **Xavier Querol:** Writing – review & editing, Supervision, Project administration, Funding acquisition, Data curation, Conceptualization.

Declaration of competing interest

The authors declare that they have no known competing financial interests or personal relationships that could have appeared to influence the work reported in this paper.

Data availability

Data will be made available on request.

Acknowledgements

This study is supported by the RI-URBANS project (Research Infrastructures Services Reinforcing Air Quality Monitoring Capacities in European Urban & Industrial Areas, European Union's Horizon 2020 research and innovation program, Green Deal, European Commission, contract 101036245), the "Agencia Estatal de Investigación" from the Spanish Ministry of Science and Innovation, FEDER funds under the projects CAIAC (PID2019-108990RB-I00), and the Generalitat de Catalunya (AGAUR 2021 SGR 00447). Additional support through Academy of Finland flagship "Atmosphere and Climate Competence Center (ACCC), grant number 337549 and 337552 as well as Technology Industries of Finland Centennial foundation via "Urbaani ilmanlaatu 2.0". This study is also part funded by the National Natural Science

Foundation of China (42101470, 72242106, 42205099), the Chunhui Project Foundation of the Education Department of China (HZKY20220053), Project of Social Science Foundation of Xinjiang Uygur Autonomous Region (2023BTY128), and Natural Science Foundation of Xinjiang Uygur Autonomous Region (2023D01A57). The authors would like to thank AtmoGrand Est for providing the data for Strasbourg and Reims; Atmo Normandie for the Gonfreville l'Orcher Petit Queuvilly and Rouen data; Atmo Nouvelle Aquitaine for the Niort - Venise, Bourdeaux - Gautier; et Poitiers - Le Nain data, and the NERC project OSCA (NE/T001976/1). This work was also supported by Natural Environment Research Council Grant NE/T001909/02, and part funded by the National Institute for Heart Research (NIHR) Health Protection Research Unit in Environmental Exposures and Health, a partnership between the UK Health Security Agency (UKHSA) and Imperial College London. We also thank Prof William Bloss for access to the Birmingham Air Quality Supersite measurements.

Appendix A. Supplementary data

Supplementary data to this article can be found online at https://doi.org/10.1016/j.envint.2024.108519.

References

Amato, F., Alastuey, A., Karanasiou, A., Lucarelli, F., Nava, S., Calzolai, G., Severi, M., Becagli, S., Gianelle, V.L., Colombi, C., 2016. AIRUSE-LIFE+: a harmonized PM speciation and source apportionment in 5 Southern European cities. Atmos. Chem. Phys. 15, 23989–24039.

Baer, D.S., Paul, J.B., Gupta, M., Keefe, O., A.,, 2002. Sensitive absorption measurements in the near-infrared region using off-axis integrated-cavity-output spectroscopy. Appl. Phys. B 75, 261–265.

Balduzzi, S., Rücker, G., Schwarzer, G., 2019. How to perform a meta-analysis with R: a practical tutorial. BMJ Ment Health 22, 153–160.

Banzhaf, S., Schaap, M., Wichink Kruit, R.J., Denier Van Der Gon, H., Stern, R., Builtjes, P., 2013. Impact of emission changes on secondary inorganic aerosol episodes across Germany. Atmos. Chem. Phys. 13, 11675–11693.

Behera, S.N., Sharma, M., 2011. Degradation of SO2, NO2 and NH3 leading to formation of secondary inorganic aerosols: an environmental chamber study. Atmos. Environ. 1994 (45), 4015–4024.

Behera, S.N., Sharma, M., Aneja, V.P., Balasubramanian, R., 2013. Ammonia in the atmosphere: a review on emission sources, atmospheric chemistry and deposition on terrestrial bodies. Environ. Sci. Pollut. Res. Int. 20, 8092–8131.

Bressi, M., Cavalli, F., Putaud, J., Fröhlich, R., Petit, J., Aas, W., Äijälä, M., Alastuey, A., Allan, J.D., Aurela, M., 2021. A European aerosol phenomenology-7: High-time resolution chemical characteristics of submicron particulate matter across Europe. Atmos. Environ. X 10, 100108.

Cape, J.N., Van der Eerden, L.J., Sheppard, L.J., Leith, I.D., Sutton, M.A., 2009. Evidence for changing the critical level for ammonia. Environ. Pollut. 157, 1033–1037.

Carslaw, D.C., Ropkins, K., 2012. Openair—an R package for air quality data analysis. Environ. Model Softw. 27, 52–61.

Chang, Y., Zou, Z., Deng, C., Huang, K., Collett, J.L., Lin, J., Zhuang, G., 2016. The importance of vehicle emissions as a source of atmospheric ammonia in the megacity of Shanghai. Atmos. Chem. Phys. 16, 3577–3594.

Chen, G., Canonaco, F., Tobler, A., Aas, W., Alastuey, A., Allan, J., Atabakhsh, S., Aurela, M., Baltensperger, U., Bougiatioti, A., 2022. European aerosol phenomenology– 8: Harmonised source apportionment of organic aerosol using 22 Year-long ACSM/AMS datasets. Environ. Int. 166, 107325.

Chen, D.D., Peace, K.E., 2013. Applied meta-analysis with R. Crc press.

Day, D.E., Chen, X., Gebhart, K.A., Carrico, C.M., Schwandner, F.M., Benedict, K.B., Schichtel, B.A., Collett Jr, J.L., 2012. Spatial and temporal variability of ammonia and other inorganic aerosol species. Atmos. Environ. 1994 (61), 490–498.

Duncan, D.B., 1955. Multiple range and multiple F tests. Biometrics 11, 1–42.

EEA, 2022. Sources and emissions of air pollutants in Europe. https://www.eea.europa.eu/publications/air-quality-in-europe-2022/sources-and-emissions-of-air.

EMEP-CEIP, 2023. EMEP Centre on Emission Inventories and Projections. Official Emission Inventories, Data Viewer https://www.ceip.at/data-viewer-2/overview-dataviewers.

H. Fagerli, S. Tsyro, D., Simpson, A., Nyíri, P., Wind, M., Gauss, A., Benedictow, H., Klein, A., Valdebenito, Q., Mu, E.G., Waersted, J., Gliß, H., Brenna, A., Mortier, J., Griesfeller, W., Aas, A., Hjellbrekke, S., Solberg, K., Tørseth, K.E., Yttri, K., Mareckova, B., Matthews, S., Schindlbacher, B., Ullrich, R., Wankmüller, T., Scheuschner, J., Kuenen, J.P., 2021. Transboundary Particulate Matter, Photo-Oxidants, Acidifying and Eutrophying Components.

Farren, N.J., Davison, J., Rose, R.A., Wagner, R.L., Carslaw, D.C., 2021. Characterisation of ammonia emissions from gasoline and gasoline hybrid passenger cars. Atmos. Environ. X 11, 100117.

Ferm, M., 1998. Atmospheric ammonia and ammonium transport in Europe and critical loads: a review. Nutr. Cycl. Agroecosyst. 51, 5–17.

Florido, E., Castaño, O., Troncoso, A., Martínez-Álvarez, F., 2015. Data mining for predicting traffic congestion and its application to Spanish data., 10th international conference on soft computing models in industrial and environmental applications. Springer, pp. 341–351.

Frey, H.C., 2018. Trends in onroad transportation energy and emissions. J. Air Waste Manag. Assoc. 68, 514–563.

Gabarrón, M., Faz, A., Acosta, J.A., 2017. Effect of different industrial activities on heavy metal concentrations and chemical distribution in topsoil and road dust. Environ. Earth Sci. 76, 1–13.

Gilbert, R.O., 1987. Statistical methods for environmental pollution monitoring. John Wiley & Sons, p. 320 p,.

Grange, S.K., Sintermann, J., Hueglin, C., 2023. Meteorologically normalised long-term trends of atmospheric ammonia (NH3) in Switzerland/Liechtenstein and the explanatory role of gas-aerosol partitioning. Sci. Total Environ. 900, 165844.

Grindlay, A.L., Martínez-Hornos, S., 2017. City-port relationships in Málaga, Spain: Effects of the new port proposals on urban traffic. WIT Transactions on the Built Environment: Urban Transport XXIII; Ricci, S., Brebbia, CA, Eds, 45-56.

GSTC, 2018. Worldwide Syngas Database. Retrieved from GSTC website on February 2. https://www.globalsyngas.org/uploads/downloads/2018-presentations/1-3HigmanGSTC2018.pdf.

Gu, B., Sutton, M.A., Chang, S.X., Ge, Y., Chang, J., 2014. Agricultural ammonia emissions contribute to China's urban air pollution. Front. Ecol. Environ. 12, 265–266.

Hellsten, S., Dragosits, U., Place, C.J., Misselbrook, T.H., Tang, Y.S., Sutton, M.A., 2007. Modelling seasonal dynamics from temporal variation in agricultural practices in the UK ammonia emission inventory. Acid Rain-Deposition to Recovery 3–13.

Hellsten, S., Dragosits, U., Place, C.J., Vieno, M., Dore, A.J., Misselbrook, T.H., Tang, Y. S., Sutton, M.A., 2008. Modelling the spatial distribution of ammonia emissions in the UK. Environ. Pollut. 154, 370–379.

Hopke, P.K., Querol, X., 2022. Is Improved Vehicular NOx Control Leading to Increased Urban NH3 Emissions? Environ. Sci. Tech. 56, 11926–11927.

Ifdc, 2016. Worldwide Ammonia Capacity Listing by Plant. Report No. IFDC-FSR-10.

In'T Veld, M., Pandolfi, M., Amato, F., Perez, N., Reche, C., Dominutti, P., Jaffrezo, J., Alastuey, A., Querol, X., Uzu, G., 2023. Discovering oxidative potential (OP) drivers of atmospheric PM10, PM2. 5, and PM1 simultaneously in North-Eastern Spain. Sci Total Environ 857, 159386.

In'T Veld, M., Seco, R., Reche, C., Pérez, N., Alastuey, A., Estrada-Portillo, M., Janssens, I.A., Peñuelas, J., Fernandez-Martinez, M., Marchand, N., 2023b. Identification of volatile organic compounds and their sources driving ozone and secondary organic aerosol formation in NE Spain. Sci. Total Environ. 167159.

Jeon, J., Lee, J.T., Park, S., 2016. Nitrogen compounds (NO, NO2, N2O, and NH3) in NO x emissions from commercial EURO VI Type heavy-duty diesel engines with a urea-selective catalytic reduction system. Energy Fuels 30, 6828–6834.

Jonson, J.E., Fagerli, H., Scheuschner, T., Tsyro, S., 2022. Modelling changes in secondary inorganic aerosol formation and nitrogen deposition in Europe from 2005 to 2030. Atmos. Chem. Phys. 22, 1311–1331.

Kendall, M.G., 1948. Rank correlation methods, 4th Edition. Charles Griffin, London.

Kirkby, J., Curtius, J., Almeida, J., Dunne, E., Duplissy, J., Ehrhart, S., Franchin, A., Gagné, S., Ickes, L., Kürten, A., 2011. Role of sulphuric acid, ammonia and galactic cosmic rays in atmospheric aerosol nucleation. Nature 476, 429–433.

Kruskal, W.H., Wallis, W.A., 1952. Use of Ranks in One-Criterion Variance Analysis. J Am Stat Assoc 47, 583–621.

Lelieveld, J., Evans, J.S., Fnais, M., Giannadaki, D., Pozzer, A., 2015. The contribution of outdoor air pollution sources to premature mortality on a global scale. Nature 525, 367–371.

Liu, X., Hadiatullah, H., Schnelle-Kreis, J., Xu, Y., Yue, M., Zhang, X., Querol, X., Cao, X., Bendl, J., Cyrys, J., 2022. Levels and drivers of urban black carbon and health risk assessment during pre-and COVID19 lockdown in Augsburg, Germany. Environ. Pollut. 120529.

Lloyd Hughes, B., Saunders, M.A., 2002. Seasonal prediction of European spring precipitation from El Niño-Southern Oscillation and local sea-surface temperatures. Int. J. Climatol. 22, 1–14.

Löflund, M., Kasper-Giebl, A., Stopper, S., Urban, H., Biebl, P., Kirchner, M., Braeutigam, S., Puxbaum, H., 2002. Monitoring ammonia in urban, inner alpine and pre-alpine ambient air. J. Environ. Monit. 4, 205–209.

Makkonen, U., Virkkula, A., Mäntykenttä, J., Hakola, H., Keronen, P., Vakkari, V., Aalto, P.P., 2012. Semi-continuous gas and inorganic aerosol measurements at a Finnish urban site: comparisons with filters, nitrogen in aerosol and gas phases, and aerosol acidity. Atmos. Chem. Phys. 12, 5617–5631.

Mann, H.B., 1945. Nonparametric tests against trend. Econometrica 245–259.

Marais, E.A., Pandey, A.K., Van Damme, M., Clarisse, L., Coheur, P.F., Shephard, M.W., Cady Pereira, K.E., Misselbrook, T., Zhu, L., Luo, G., 2021. UK ammonia emissions estimated with satellite observations and GEOS-Chem. J. Geophys. Res. Atmos. 126, e2021J–e35237J.

Massagué, J., Escudero, M., Alastuey, A., Mantilla, E., Monfort, E., Gangoiti, G., García-Pando, C.P., Querol, X., 2023. Spatiotemporal variations of tropospheric ozone in Spain (2008–2019). Environ. Int. 176, 107961.

Misselbrook, T.H., Sutton, M.A., Scholefield, D., 2004. A simple process-based model for estimating ammonia emissions from agricultural land after fertilizer applications. Soil Use Manage. 20, 365–372.

Nguyen, D.V., Sato, H., Hamada, H., Yamaguchi, S., Hiraki, T., Nakatsubo, R., Murano, K., Aikawa, M., 2021. Symbolic seasonal variation newly found in atmospheric ammonia concentration in urban area of Japan. Atmos Environ (1994) 244, 117943.

Ni, J.Q., Heber, A.J., Lim, T.T., Diehl, C.A., Duggirala, R.K., Haymore, B.L., Sutton, A.L., 2000. Ammonia emission from a large mechanically-ventilated swine building during warm weather. Wiley Online Library.

Norman, M., Spirig, C., Wolff, V., Trebs, I., Flechard, C., Wisthaler, A., Schnitzhofer, R., Hansel, A., Neftel, A., 2009. Intercomparison of ammonia measurement techniques at an intensively managed grassland site (Oensingen, Switzerland). Atmos. Chem. Phys. 9, 2635–2645.
Pandolfi, M., Amato, F., Reche, C., Alastuey, A., Otjes, R.P., Blom, M.J., Querol, X., 2012. Summer ammonia measurements in a densely populated Mediterranean city. Atmos. Chem. Phys. 12, 7557–7575.
Pasini, C., 2022. Conflitti aliEni. Raffineria e territorio a Sannazzaro de'Burgondi. ZAPRUDER, 106-116.
Paulot, F., Jacob, D.J., Pinder, R.W., Bash, J.O., Travis, K., Henze, D.K., 2014. Ammonia emissions in the United States, European Union, and China derived by high-resolution inversion of ammonium wet deposition data: Interpretation with a new agricultural emissions inventory (MASAGE_NH3). J. Geophys. Res. Atmos. 119, 4343–4364.
Pinho, P., Branquinho, C., Cruz, C., Tang, Y.S., Dias, T., Rosa, A.P., Máguas, C., Martins-Loução, M., Sutton, M.A., 2009. Assessment of critical levels of atmospheric ammonia for lichen diversity in cork-oak woodland, Portugal. Atmos. Ammonia 109–119.
Reche, C., Viana, M., Pandolfi, M., Alastuey, A., Moreno, T., Amato, F., Ripoll, A., Querol, X., 2012. Urban NH3 levels and sources in a Mediterranean environment. Atmos. Environ. 1994 (57), 153–164.
Reche, C., Viana, M., Karanasiou, A., Cusack, M., Alastuey, A., Artiñano, B., Revuelta, M. A., López-Mahía, P., Blanco-Heras, G., Rodríguez, S., 2015. Urban NH3 levels and sources in six major Spanish cities. Chemosphere 119, 769–777.
Reche, C., Perez, N., Alastuey, A., Cots, N., Pérez, E., Querol, X., 2022. 2011–2020 trends of urban and regional ammonia in and around Barcelona. NE Spain. Chemosphere 304, 135347.
Rumsey, I.C., Cowen, K.A., Walker, J.T., Kelly, T.J., Hanft, E.A., Mishoe, K., Rogers, C., Proost, R., Beachley, G.M., Lear, G., 2014. An assessment of the performance of the Monitor for AeRosols and GAses in ambient air (MARGA): a semi-continuous method for soluble compounds. Atmos. Chem. Phys. 14, 5639–5658.
Saiz-Lopez, A., Adame, J.A., Notario, A., Poblete, J., Bolívar, J.P., Albaladejo, J., 2009. Year-round observations of NO, NO 2, O 3, SO 2, and Toluene measured with a DOAS system in the industrial area of Puertollano, Spain. Water Air Soil Pollut. 200, 277–288.
Salmi, T., Määttä, A., Anttila, P., Ruoho-Airola, T., Amnell, T., 2002. Detecting Trends of Annual Values of Atmospheric Pollutants by the Mann-Kendall Test and Sen's Slope Estimates-the Excel Template Application MAKESENS. Publications on Air Quality, n.31 Finnish Meteorological Institute 35, p.
Saraswati, S., Mandal, T.K., 2018. Five-year measurements of ambient ammonia and its relationships with other trace gases at an urban site of Delhi, India. Meteorol. Atmos. Phys. 130, 241–257.
Sharma, S.K., Datta, A., Saud, T., Mandal, T.K., Ahammed, Y.N., Arya, B.C., Tiwari, M.K., 2010. Study on concentration of ambient NH 3 and interactions with some other ambient trace gases. Environ. Monit. Assess. 162, 225–235.
Shephard, M.W., Dammers, E., Cady-Pereira, K.E., Kharol, S.K., Thompson, J., Gainariu-Matz, Y., Zhang, J., McLinden, C.A., Kovachik, A., Moran, M., 2020. Ammonia measurements from space with the Cross-track Infrared Sounder: characteristics and applications. Atmos. Chem. Phys. 20, 2277–2302.
Silvaggio, R., Curcuruto, S., Mazzocchi, E., Borchi, F., Bartalucci, C., Governi, L., Carfagni, M., Bellomini, R., Luzzi, S., Colucci, G., 2020. Life Monza: Comparison between ante and post-operam noise and air quality monitoring activities in a Noise Low Emission Zone. Noise Mapp 7, 171–191.
Singh, R., Kim, K., Park, G., Kang, S., Park, T., Ban, J., Choi, S., Song, J., Yu, D., Woo, J., 2021. Seasonal and Spatial Variations of Atmospheric Ammonia in the Urban and Suburban Environments of Seoul. Korea. Atmosphere (basel) 12, 1607.
Song, X., Naber, J.D., Johnson, J.H., 2015. A study of the effects of NH3 maldistribution on a urea-selective catalytic reduction system. Int. J. Engine Res. 16, 213–222.
Suarez-Bertoa, R., Mendoza-Villafuerte, P., Riccobono, F., Vojtisek, M., Pechout, M., Perujo, A., Astorga, C., 2017. On-road measurement of NH3 emissions from gasoline and diesel passenger cars during real world driving conditions. Atmos. Environ. 1994 (166), 488–497.
Sutton, M. A., Howard, C. M., Mason, K. E., Brownlie, W. J., Cordovil, C. M. d. S. (eds.), 2022. Nitrogen Opportunities for Agriculture, Food & Environment. UNECE Guidance Document on Integrated Sustainable Nitrogen Management. UK Centre for Ecology & Hydrology, Edinburgh, UK.
Sutton, M.A., Place, C.J., Eager, M., Fowler, D., Smith, R.I., 1995. Assessment of the magnitude of ammonia emissions in the United Kingdom. Atmos. Environ. 1994 (29), 1393–1411.
Sutton, M.A., Tang, Y.S., Dragosits, U., Fournier, N., Dore, A.J., Smith, R.I., Weston, K.J., Fowler, D., 2001. A spatial analysis of atmospheric ammonia and ammonium in the UK. Scientific World Journal 1, 275–286.
Tang, Y.S., Braban, C.F., Dragosits, U., Dore, A.J., Simmons, I., van Dijk, N., Poskitt, J., Dos Santos Pereira, G., Keenan, P.O., Conolly, C., 2018. Drivers for spatial, temporal and long-term trends in atmospheric ammonia and ammonium in the UK. Atmos. Chem. Phys. 18, 705–733.
Tang, Y.S., Flechard, C.R., Dämmgen, U., Vidic, S., Djuricic, V., Mitosinkova, M., Uggerud, H.T., Sanz, M.J., Simmons, I., Dragosits, U., 2021. Pan-European rural monitoring network shows dominance of NH 3 gas and NH 4 NO 3 aerosol in inorganic atmospheric pollution load. Atmos. Chem. Phys. 21, 875–914.
Tichý, O., Eckhardt, S., Balkanski, Y., Hauglustaine, D., Evangeliou, N., 2023. Decreasing trends of ammonia emissions over Europe seen from remote sensing and inverse modelling. Egusphere 2023, 1–30.
Twigg, M.M., Di Marco, C.F., Leeson, S., Van Dijk, N., Jones, M.R., Leith, I.D., Morrison, E., Coyle, M., Proost, R., Peeters, A., 2015. Water soluble aerosols and gases at a UK background site–Part 1: Controls of PM 2.5 and PM 10 aerosol composition. Atmos. Chem. Phys. 15, 8131–8145.
Twigg, M.M., Berkhout, A.J., Cowan, N., Crunaire, S., Dammers, E., Ebert, V., Gaudion, V., Haaima, M., Häni, C., John, L., 2022. Intercomparison of in situ measurements of ambient NH 3: instrument performance and application under field conditions. Atmos. Meas. Tech. 15, 6755–6787.
UAR, 2023. Urban Access Regulations. https://urbanaccessregulations.eu/.
UNECE, 2007. Review of the 1999 Gothenburg Protocol. Report on the Workshop on Atmospheric Ammonia: Detecting Emission Changes and Environmental Impacts. Report to the 39th Session of the Working Group on Strategies and Review. ECE/EB. AIR/WG.5/2007/3.
Vaittinen, O., Metsälä, M., Halonen, L., Persijn, S., Leuenberger, D., Niederhauser, B., 2018. Effect of moisture on the adsorption of ammonia. Appl. Phys. B 124, 1–8.
Van Damme, M., Clarisse, L., Whitburn, S., Hadji-Lazaro, J., Hurtmans, D., Clerbaux, C., Coheur, P., 2018. Industrial and agricultural ammonia point sources exposed. Nature 564, 99–103.
Van Damme, M., Clarisse, L., Franco, B., Sutton, M.A., Erisman, J.W., Kruit, R.W., Van Zanten, M., Whitburn, S., Hadji-Lazaro, J., Hurtmans, D., 2021. Global, regional and national trends of atmospheric ammonia derived from a decadal (2008–2018) satellite record. Environ. Res. Lett. 16, 55017.
Wang, C., Li, X., Zhang, T., Tang, A., Cui, M., Liu, X., Ma, X., Zhang, Y., Liu, X., Zheng, M., 2022. Developing Nitrogen Isotopic Source Profiles of Atmospheric Ammonia for Source Apportionment of Ammonia in Urban Beijing. Front. Environ. Sci. 10, 903013.
Wang, Y., Zhang, Q.Q., He, K., Zhang, Q., Chai, L., 2013. Sulfate-nitrate-ammonium aerosols over China: response to 2000–2015 emission changes of sulfur dioxide, nitrogen oxides, and ammonia. Atmos. Chem. Phys. 13, 2635–2652.
Winkler, R., Adamsen, A.P.S., 2017. Ammonia emissions from air cleaners at pig farms in Denmark using a Picarro cavity ring-down spectrometer., EGU General Assembly Conference Abstracts, p. 9343.
Wu, G., Wang, H., Zhang, C., Gong, D., Liu, X., Ristovski, Z., Wang, B., 2023. Anthropogenic pollutants induce enhancement of aerosol acidity at a mountainous background atmosphere in southern China. Sci. Total Environ. 903, 166192.
Wyer, K.E., Kelleghan, D.B., Blanes-Vidal, V., Schauberger, G., Curran, T.P., 2022. Ammonia emissions from agriculture and their contribution to fine particulate matter: A review of implications for human health. J. Environ. Manage. 323, 116285.
Yao, X., Zhang, L., 2016. Trends in atmospheric ammonia at urban, rural, and remote sites across North America. Atmos. Chem. Phys. 16, 11465–11475.
Zhang, X., Lin, W., Ma, Z., Xu, X., 2021. Indoor NH3 variation and its relationship with outdoor NH3 in urban Beijing. Indoor Air 31, 2130–2141.
Zhou, C., Zhou, H., Holsen, T.M., Hopke, P.K., Edgerton, E.S., Schwab, J.J., 2019. Ambient ammonia concentrations across New York state. J. Geophys. Res. Atmos. 124, 8287–8302.